Hindawi Publishing Corporation
Advances in Astronomy
Volume 2010, Article ID 162083, 15 pages
doi:10.1155/2010/162083

Review Article

The Dark Matter Annihilation Signal from Dwarf Galaxies and Subhalos

Michael Kuhlen

School of Natural Science, Institute for Advanced Study, Einstein Lane, Princeton, NJ 08540, USA

Correspondence should be addressed to Michael Kuhlen, mqk@astro.berkeley.edu

Received 8 June 2009; Accepted 13 August 2009

Academic Editor: Andrey V. Kravtsov

Dark Matter annihilation holds great potential for directly probing the clumpiness of the Galactic halo that is one of the key predictions of the Cold Dark Matter paradigm of hierarchical structure formation. Here we review the γ-ray signal arising from dark matter annihilation in the centers of Galactic subhalos. We consider both known Galactic dwarf satellite galaxies and dark clumps without a stellar component as potential sources. Utilizing the *Via Lactea II* numerical simulation, we estimate fluxes for 18 Galactic dwarf spheroidals with published central densities. The most promising source is Segue 1, followed by Ursa Major II, Ursa Minor, Draco, and Carina. We show that if any of the known Galactic satellites can be detected, then at least ten times more subhalos should be visible, with a significant fraction of them being dark clumps.

1. Introduction

A decade has gone by since the emergence of the "Missing Satellite Problem" [1, 2], which refers to the apparent discrepancy between the observed number of Milky Way satellite galaxies, 23 by latest count [3–12], and the predicted number of dark matter (DM) subhalos that should be orbiting in the Milky Way's halo. The latest cosmological numerical simulations [13–15] resolve close to 100,000 individual self-bound clumps of DM within the Galactic virial volume—remnants of the hierarchical build-up of the Milky Way's DM halo. Several hundred of these may be large enough to host a dwarf galaxy. A consensus seems to be emerging that this discrepancy is not a short-coming of the otherwise tremendously successful Cold Dark Matter (CDM) hypothesis [16, 17], but instead reflects the complicated baryonic physics that determines which subhalos are able to host a luminous stellar component and which are not [18–24]. If this explanation is correct, then an immediate consequence is that the Milky Way dark halo should be filled with clumps on all scales down to the CDM free-streaming scale at 10^{-12} to $10^{-4}\,M_\odot$ for cold thermal relics (e.g., supersymmetric CDM) [25–28] or as low as $\sim 10^{-20}\,M_\odot$ in the case of non-thermal cold axions [29–31]. At the moment there is little empirical evidence for or against this prediction, and this has motivated searches for new signals that could provide tests of this hypothesis, and ultimately help to constrain the nature of the DM particle.

One of the most promising such signals is DM annihilation [32]. In regions of sufficiently high density, for example in the centers of Galactic subhalos, the DM pair annihilation rate might become large enough to allow for a detection of neutrinos, energetic electrons and positrons, or γ-ray photons, which are the by-products of the annihilation process. This is one of the few ways in which the dark sector can be coupled to ordinary matter and radiation amenable to astronomical observation. Belying its commonly used name of "indirect detection", DM annihilation is really the only way we can hope to directly probe the clumpiness of the Galactic DM distribution. One could argue that it is a more "direct" method than trying to constrain DM clumpiness from its effects on strong gravitational lensing (see Zackrisson & Riehm's contribution in this special edition), or from the kinematics of stars orbiting in DM-dominated potentials [33], or from perturbations of cold stellar structures like globular cluster tidal streams [34–37] or the heating of the Milky Way's stellar disk [38–40], although all of these are also worthwhile approaches to take.

The only trouble with the DM annihilation signal is that so far there have been no undisputed claims of its detection.

Recently there have been several reports of "anomalous" features in the local cosmic ray flux: the PAMELA satellite reported an increasing positron fraction at energies between 10 and 100 GeV [41], where standard models of cosmic ray propagation predict a decreasing fraction; the ATIC [42] and PPB-BETS [43] balloon-borne experiments reported a surprisingly large total electron and positron flux at ~500 GeV, although recent *Fermi* [44] and H.E.S.S. data [45] appear to be inconsistent with it. Either of these cosmic ray anomalies might be the long sought after signature of local DM annihilation. However, since the currently available data can equally well be explained by conventional astrophysical sources (e.g., nearby pulsars or supernova remnants), they hardly provide incontrovertible evidence for DM annihilation. The next few years hold great potential for progress, since the recently launched *Fermi Gamma-ray Space Telescope* will conduct a blind survey of the γ-ray sky at unprecedented sensitivity, energy extent, and angular resolution. At the same time, Atmospheric Cerenkov Telescopes, such as H.E.S.S., VERITAS, MAGIC, and STACEE, are greatly increasing their sensitivity, and have only recently begun to search for a DM annihilation signal from the centers of nearby dwarf satellite galaxies [46–50].

The purpose of this paper is to provide an overview of the potential DM annihilation signal from individual Galactic DM subhalos, either as dwarf satellite galaxies or as dark clumps. It does not cover a number of very interesting and closely related topics, which are actively being researched and deserve to be examined in equal detail. These include the diffuse flux from Galactic substructure and its anisotropies (e.g., [51–53]), the relative strength of the signal from individual subhalos compared with that from the Galactic Center or an annulus around it [54, 55], the effect of a nearby DM subhalo on the amplitude and spectrum of the local high energy electron and positron flux [56, 57], and the role of the Sommerfeld enhancement [58] on the DM annihilation rate and its implications for substructure signals [59–61].

This paper is organized as follows: we first review the basic physics of DM annihilation, briefly touching on the relic density calculation, the "WIMP miracle", DM particle candidates, and, in more detail, the sources of γ-rays from DM annihilation. In the following section we review what numerical simulations have revealed about the basic properties of DM subhalos that are relevant for the annihilation signal. We go on to consider known Milky Way dwarf spheroidal galaxies as sources, using the *Via Lactea II* simulation to infer the most likely annihilation fluxes from published values of the dwarfs' central masses. Next we discuss the possibility of a DM annihilation signal from dark clumps, halos that have too low a mass to host a luminous stellar component. Lastly, we briefly discuss the role of the substructure boost factor for the detectability of individual DM subhalos.

2. Dark Matter Annihilation

If DM is made up of a so-called "thermal relic" particle, (An alternative DM candidate is the axion, a non-thermal relic particle motivated as a solution to the strong CP problem [62]. Since it does not produce an annihilation signal today, we do not further consider it here.) its abundance today is set by its annihilation cross section in the early universe. The thermal relic abundance calculation relating today's abundance of DM to the properties of the DM particle (its mass and annihilation cross section) is straightforward and elegant, and has been described in pedagogical detail previously [63–65]. We briefly summarize the story here.

At sufficiently early times, the DM particles are in thermal equilibrium with the rest of the universe. As long as they remain relativistic ($T \gg m_\chi$), their creation and destruction rates are balanced, and hence their comoving abundance remains constant. Once the universe cools below the DM particle's rest-mass ($T < m_\chi$), its equilibrium abundance is suppressed by a Boltzmann factor $\exp(-m_\chi/T)$. If equilibrium had been maintained until today, the DM particles would have completely annihilated away. Instead the expansion of the universe comes to the rescue and causes the DM particles to fall out of equilibrium once the expansion rate (given by $H(a)$, the Hubble constant at cosmological scale factor a) exceeds the annihilation rate $\Gamma(a) = n\langle\sigma v\rangle$, that is, when DM particles can no longer find each other to annihilate. The comoving number density of DM particles is then fixed at a "freeze-out" temperature that turns out to be approximately $T_f \simeq m_\chi/20$, with only a weak additional logarithmic dependence on the mass and cross section of the DM particle. A back of the envelope calculation results in the following relation between Ω_χ, the relic mass density in units of the critical density of the universe $\rho_{\rm crit} = 3H_0^2/8\pi G$, and $\langle\sigma v\rangle$, the thermally averaged velocity-weighted annihilation cross section:

$$\omega_\chi = \Omega_\chi h^2 = \frac{3\times 10^{-27}\,\mathrm{cm^3\,s^{-1}}}{\langle\sigma v\rangle}. \quad (1)$$

Note that this relation is independent of m_χ. The WMAP satellite's measurement of the DM density is $\omega_\chi = 0.1131 \pm 0.0034$ [66], implying a value of

$$\langle\sigma v\rangle \approx 3\times 10^{-26}\,\mathrm{cm^3\,s^{-1}}. \quad (2)$$

A more accurate determination of $\langle\sigma v\rangle$ must rely on a numerical solution of the Boltzmann equation in an expanding universe, taking into account the full temperature dependence of the annihilation rate, including the possibilities of resonances and coannihilations into other, nearly degenerate dark sector particles (e.g., [67, 68]). It is a remarkable coincidence that this value of $\langle\sigma v\rangle$ is close to what one expects for a cross section set by the weak interaction. This is the so-called "WIMP miracle", and it is the main motivation for considering weakly interacting massive particles (WIMPs) as prime DM candidates.

The Standard Model of particle physics actually provides one class of WIMPs, massive neutrinos. Although neutrinos thus constitute a form of DM, they cannot make up the bulk of it, since their small mass, $\sum m_\nu < 0.63\,\mathrm{eV}$ [66], implies a cosmological mass density of only $\omega_\nu = 7.1\times 10^{-3}$. Since the standard neutrino is a hot dark matter particle, increasing its contribution to the total matter density would

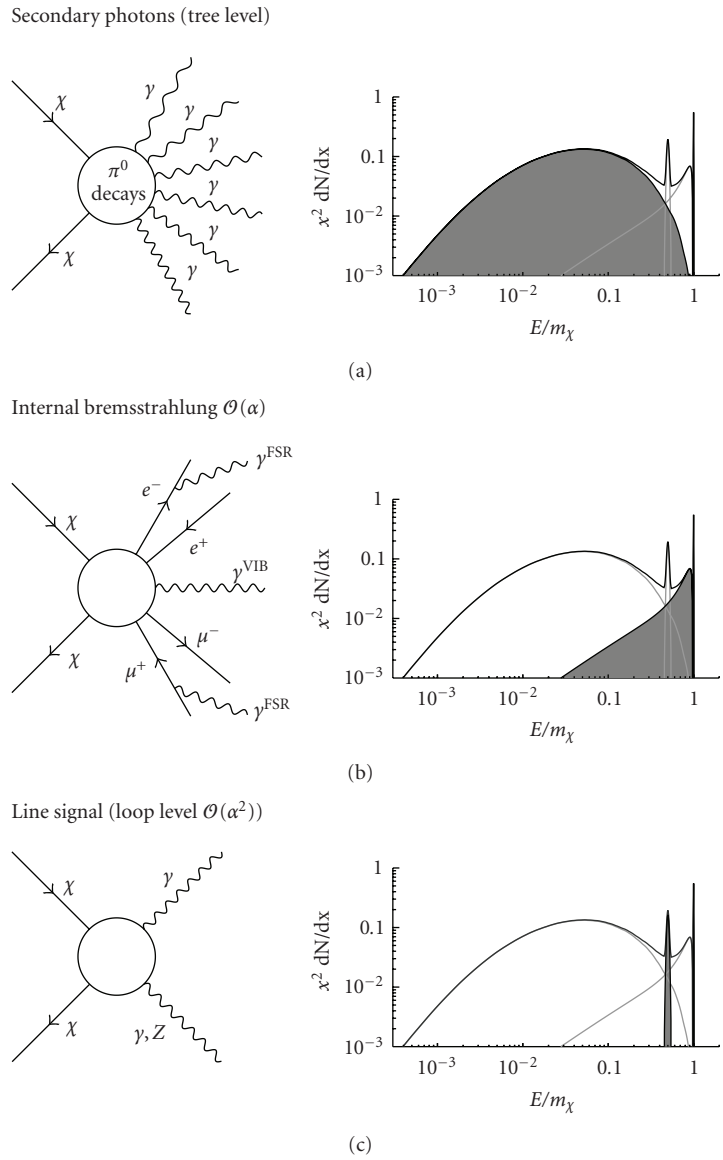

Figure 1: A schematic of the different sources and energy distributions of γ-rays from WIMP annihilation. (a) Secondary photons arising from the decay of neutral pions produced in the hadronization of primary annihilation products. (b) Internal bremsstrahlung photons associated with charged annihilation products, either in the form of final state radiation (FSR) from external legs or as virtual internal bremsstrahlung (VIB) from the exchange of virtual charged particles. (c) Monochromatic line signals from the prompt annihilation into two photons or a photon and Z boson. This process occurs only at loop level, and hence is typically strongly suppressed.

destroy small scale structure and violate constraints from galaxy clustering and the Lyman alpha forest. The attention thus turns to extensions of the Standard Model, which themselves are theoretically motivated by the hierarchy problem (the enormous disparity between the weak and Planck scales) and the quest for a unification of gravity and quantum mechanics. The most widely studied class of such models consists of supersymmetric extensions of the Standard Model. Additionally models with extra dimensions have received a lot of attention in recent years. Both of these approaches offer good DM particle candidates: the lightest supersymmetric particle (LSP), typically a *neutralino* in R-parity conserving supersymmetry, and the lightest Kaluza-Klein particle (LKP), typically the $B^{(1)}$ particle, the first Kaluza-Klein excitation of the hypercharge gauge boson, in Universal Extra Dimension models. For much more information, we recommend the comprehensive recent review of particle DM candidates by Bertone et al. [65].

The direct products of the annihilation of two DM particles are strongly model dependent. Typical channels include annihilations into charged leptons ($e^+e^-, \mu^+\mu^-$, $\tau^+\tau^-$), quark-antiquark pairs, and gauge and Higgs bosons (W^+W^-, ZZ, Zh, hh). In the end, however, the decay and hadronization of these annihilation products results in only three types of emissions: (i) high energy neutrinos and antineutrinos, (ii) relativistic electrons and protons and their antiparticles, and (iii) γ-ray photons. Additional lower energy photons can result from the interaction of

the relativistic electrons with magnetic fields (synchrotron radiation), with interstellar material (bremsstrahlung), and with the CMB and stellar radiation fields (inverse Compton scattering). In the following we will focus on the γ-rays, since they are likely the strongest signal from Galactic DM substructure. γ-rays are produced in DM annihilations in three ways (see accompanying Figure 1).

(i) Since the DM particle is neutral, there is no direct coupling to photons. Nevertheless, copious amounts of secondary γ-ray photons can be produced through the decay of neutral pions, $\pi^0 \rightarrow \gamma\gamma$, arising in the hadronization of the primary annihilation products. Since the DM particles are non-relativistic, their annihilation results in a pair of monoenergetic particles with energy equal to m_χ, which fragment and decay into π-meson dominated "jets". In this way a single DM annihilation event can produce several tens of γ-ray photons. The result is a broad spectrum with a cutoff around m_χ.

(ii) An important additional contribution at high energies ($E \lesssim m_\chi$) arises from the internal bremsstrahlung process [69], which may occur with any charged annihilation product. One can distinguish between final state radiation, in which the photon is radiated from an external leg, and virtual internal bremsstrahlung, arising from the exchange of a charged virtual particle. Note that neither of these processes requires an external electromagnetic field (hence the name *internal* bremsstrahlung). The resulting γ-ray spectrum is peaked towards $E \sim m_\chi$ and exhibits a sharp cutoff. Although it is suppressed by one factor of the coupling α compared to pion decays, it can produce a distinctive spectral feature at high energies. This could aide the confirmation of a DM annihilation nature of any source and might allow a direct determination of m_χ.

(iii) Lastly, it is possible for DM particles to directly produce γ-ray photons, but one has to go to loop-level to find contributing Feynman diagrams, and hence this flux is typically strongly suppressed by two factors of α (although exceptions exist [70]). On the other hand, the resulting photons would be monochromatic, and a detection of such a line signal would provide strong evidence of a DM annihilation origin of any signal. While annihilations directly into two photons, $\chi\chi \rightarrow \gamma\gamma$, would produce a narrow line at $E = m_\chi$, in some models it is also possible to annihilate into a photon and a Z boson, $\chi\chi \rightarrow \gamma Z$, and this process would result in a somewhat broadened (due to the mass of the Z) line at $E \sim m_\chi(1 - m_Z^2/4m_\chi^2)$.

The relative importance of these three γ-ray production channels and the resulting spectrum dN_γ/dE depend on the details of the DM particle model under consideration. For any given model, realistic γ-ray spectra can be calculated using sophisticated and publicly available computer programs, such as the PYTHIA Monte-Carlo event generator [71], which is also contained in the popular DarkSUSY package [72].

3. Dark Matter Substructure as Discrete γ-Ray Sources

DM subhalos as individual discrete γ-ray sources hold great potential for providing a "smoking gun" signature of DM annihilation [32, 54, 54, 73–83]. Compared to diffuse γ-ray annihilation signals, these discrete sources should be easier to distinguish from astrophysical backgrounds and foregrounds [84], since (a) typical astrophysical sources of high energy γ-rays, such as pulsars and supernova remnants, are very rare in dwarf galaxies, owing to their predominantly old stellar populations, (b) the DM annihilation flux should be time-independent, (c) angularly extended, and (d) not exhibit any (or only very weak) low energy emission due to the absence of strong magnetic fields or stellar radiation fields. (Inverse Compton radiation from scattering off the CMB, however, may be present.)

We can distinguish between DM subhalos hosting a Milky Way dwarf satellite galaxy and dark clumps that, for whatever reason, do not host a luminous stellar population, or one that is too faint to have been detected up to now. Before we go on to discuss the prospects of detecting a DM annihilation signal from these two classes of sources, we review the basic properties of DM subhalos common to both.

Numerical simulations have shown that pure DM (sub)halos have density profiles that are well described by a Navarro, Frenk & White (NFW) [85] profile over a wide range of masses [86, 87],

$$\rho_{\rm NFW}(r) = \frac{4\rho_s}{(r/r_s)(1 + r/r_s)^2}. \quad (3)$$

The parameter r_s indicates the radius at which the logarithmic slope $\gamma(r) \equiv d\ln\rho/d\ln r = -2$, and $\rho(r_s) = \rho_s$. The very highest resolution simulations have recently provided some indications of a flattening of the density profile in the innermost regions [15, 88]. In this case a so-called Einasto profile may provide a better overall fit,

$$\rho_{\rm Einasto}(r) = \rho_s \exp\left[-\frac{2}{\alpha}\left(\left(\frac{r}{r_s}\right)^\alpha - 1\right)\right]. \quad (4)$$

Here the additional parameter α governs how fast the profile rolls over, and has been found to have a value of $\alpha \approx 0.17 \pm 0.03$ in numerical simulations [88]. Note that the two density profiles actually do not differ very much until $r \ll r_s$ (cf. Figure 2(a)). Simulated DM halos are of course not perfectly spherically symmetric, and instead typically exhibit prolate or triaxial isodensity contours that become more elongated towards the center [89]. The degree of prolateness decreases with mass, and galactic subhalos have axis ratios of $\gtrsim 0.7$ [90].

The "virial" radius $R_{\rm vir}$ of a halo is defined as the radius enclosing a mean density equal to $\Delta_{\rm vir}\rho_0$, where $\Delta_{\rm vir} \approx 389$ (from a spherical collapse calculation [91]) and ρ_0 is the mean density of the universe. The corresponding virial mass $M_{\rm vir}$ is the mass within $R_{\rm vir}$, and a halo's concentration

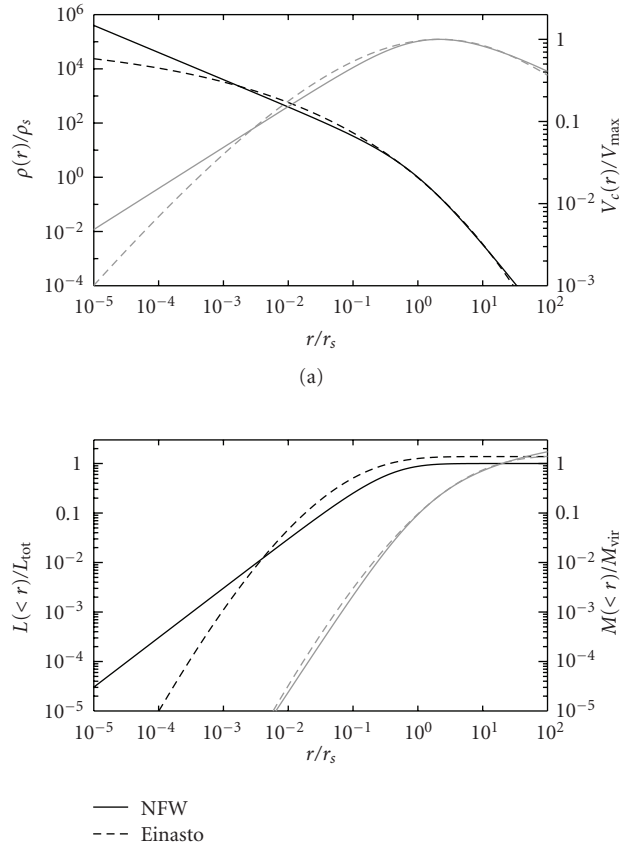

FIGURE 2: A comparison of NFW and Einasto ($\alpha = 0.17$) radial profiles of density (top, dark lines, left axis), circular velocity (top, light lines, right axis), enclosed annihilation luminosity (bottom, dark lines, left axis), enclosed mass (bottom, light lines, right axis). The density profiles have been normalized to have the same $V_{\max}$ and $r_{\rm Vmax}$.

can then be defined as $c = R_{\rm vir}/r_s$. While these quantities are well defined for isolated halos and commonly used in analytic models, they are somewhat less applicable to galactic subhalos, since the outer radius of a subhalo is set by tidal truncation, which depends on the subhalo's location within its host halo. Furthermore, in numerical simulations it is difficult to resolve r_s in low mass subhalos. For this reason we prefer to work with $V_{\max}$, the maximum of the circular velocity curve $V_c(r)^2 = GM(<r)/r$ and a proxy for a subhalo's mass, and $r_{\rm Vmax}$, the radius at which $V_{\max}$ occurs. These quantities are much more robustly determined for subhalos in numerical simulations than (M, c). Note that even $(V_{\max}, r_{\rm Vmax})$ can be affected by tidal interactions with the host halo, especially for subhalos close to the host halo center. For this reason we also sometimes consider $V_{\rm peak}$, the largest value of $V_{\max}$ that a subhalo ever acquired during its lifetime (i.e., before tidal stripping began to lower its $V_{\max}$) and $r_{\rm Vpeak}$, the corresponding radius.

Since DM annihilation is a two body process, its rate is proportional to the square of the local density, and the annihilation "luminosity" is given by the volume integral of $\rho(r)^2$,

$$\mathcal{L}(<r) \equiv \int_0^r \rho^2 dV. \tag{5}$$

$\mathcal{L}$ has dimensions of (mass)^2 (length)$^{-3}$, and we express it in units of $\mathrm{M}_\odot^2\ \mathrm{pc}^{-3}$. In order to convert to a conventional luminosity, one must multiply by a particle physics term,

$$L = c^2 \frac{\langle \sigma v \rangle}{m_\chi} \mathcal{L}, \tag{6}$$

where c is the speed of light, m_χ the mass of the DM particle and $\langle \sigma v \rangle$ the thermally averaged velocity-weighted annihilation cross section discussed in the previous section. This is the *total* luminosity, but we are interested here only in the fraction emitted as γ-rays. Furthermore, a given detector is only sensitive to γ-rays above a threshold energy of $E_{\rm th}$ and below a maximum energy of $E_{\max}$. In that case the effective γ-ray luminosity is

$$L_\gamma^{\rm eff} = \left[\frac{\langle \sigma v \rangle}{2 m_\chi^2} \int_{E_{\rm th}}^{E_{\max}} E \frac{dN_\gamma}{dE} dE \right] \mathcal{L}, \tag{7}$$

where dN_γ/dE is the spectrum of γ-ray photons produced in a single annihilation event.

A comparison of the enclosed luminosity and mass profiles is shown in the bottom panel of Figure 2. Clearly, $\mathcal{L}$ is much more centrally concentrated than M: ~90% of the total luminosity is produced within r_s, compared with only 10% of the total mass. In terms of $(V_{\max}, r_{\rm Vmax})$, the total luminosity of a halo is given by

$$\mathcal{L} = f \frac{V_{\max}^4}{G^2 r_{\rm Vmax}}, \tag{8}$$

where f is an $\mathcal{O}(1)$ numerical factor that depends on the shape of the density profile; for an NFW profile $f = 1.227$, and for an $\alpha = 0.17$ Einasto profile $f = 1.735$. In physical units, the total annihilation luminosity is

$$\mathcal{L} = \begin{matrix} 1.1 \\ 1.5 \end{matrix} \times 10^7\ \mathrm{M}_\odot^2\ \mathrm{pc}^{-3} \left(\frac{V_{\max}}{20\ \mathrm{km\ s}^{-1}} \right)^4 \left(\frac{r_{\rm Vmax}}{1\ \mathrm{kpc}} \right)^{-1}, \tag{9}$$

for NFW (top) and $\alpha = 0.17$ Einasto (bottom). Note that even though the slope of the Einasto profile is shallower than NFW in the very center, the total luminosity exceeds that of an NFW halo with the same $(V_{\max}, r_{\rm Vmax})$. This is due to the fact that the Einasto profile rolls over less rapidly than the NFW profile, and actually has slightly higher density than NFW between r_s and a cross-over point at $\sim 10^{-3} r_s$.

4. Milky Way Dwarf Spheroidal Galaxies

There are several advantages of known dwarf satellite galaxies as DM annihilation sources: firstly, the kinematics of individual stars imply mass-to-light ratios of up to several hundred [92–95], and hence there is an a priori expectation of high DM densities; secondly, since we know their location

in the sky, it is possible to directly target them with sensitive atmospheric Cerenkov telescopes (ACT) such as H.E.S.S., VERITAS, MAGIC, and STACEE, whose small field of view makes blind searches impractical; lastly, our approximate knowledge of the distances to many dwarf satellites would allow a determination of the absolute annihilation rate, which may lead to a direct constraint on the annihilation cross section, if the DM particle mass can be independently measured (from the shape of the spectrum, e.g.).

Recent observational progress utilizing the Sloan Digital Sky Survey (SDSS) has more than doubled the number of known dwarf spheroidal (dSph) satellite galaxies orbiting the Milky Way [4–12], raising the total from the 9 "classical" ones to 23. Many of the newly discovered satellites are so-called "ultra-faint" dSph's, with luminosities as low as $1,000 L_\odot$ and only tens to hundreds of spectroscopically confirmed member stars. Simply accounting for the SDSS sky coverage (about 20%), the total number of luminous Milky Way satellites can be estimated to be at least 70. Taking into account the SDSS detection limits [96] and a radial distribution of DM subhalos motivated by numerical simulations, this estimate can grow to several hundreds of satellite galaxies in total [97, 98].

In order to assess the strength of the DM annihilation signal from these dSph's, it is necessary to have an estimate of the total dynamical mass, or at least $V_{\rm max}$, of the DM halo hosting the galaxies. Owing to the extreme faintness of these objects and their lack of a detectable gaseous component [99], it has been very difficult to obtain kinematic information that allows for such measurements. Progress has been made through spectroscopic observations of individual member stars, whose line-of-sight velocity dispersions have confirmed that these objects are in fact strongly DM dominated [92–95]. Such data best constrain the enclosed dynamical mass within the stellar extent, which on average is about 0.3 kpc for current data sets. A recent analysis has determined $M_{0.3} \equiv M(< 0.3\,\text{kpc})$ for 18 of the Milky Way dSph's, and found that, surprisingly, they all have $M_{0.3} \approx 10^7\,\text{M}_\odot$ to within a factor of two [33]. At present the physical meaning of this mass scale is unclear, but it may provide a clue to the nature of the baryonic processes that govern dwarf galaxy formation.

State-of-the-art cosmological numerical simulations of the formation of the DM halo of a Milky Way scale galaxy, such as those of the Via Lactea Project [13, 80] and the Aquarius Project [14], have now reached an adequate mass and force resolution to directly determine $M_{0.3}$ in their simulated subhalos. This makes it possible to infer the most likely values of $(V_{\rm max}, r_{\rm Vmax})$ for a Milky Way dSph of a given $M_{0.3}$ and Galacto-centric distance D, by identifying all simulated subhalos with comparable $M_{0.3}$ and D and averaging over their $(V_{\rm max}, r_{\rm Vmax})$. This analysis was performed for the 9 "classical" dwarfs using the *Via Lactea I* simulation [22], and we extend it here to all 18 dwarfs published in [33] and with the more recent and higher resolution *Via Lactea II* (VL2) simulation.

For each of the Milky Way dSph's studied in [33] we created a list of all VL2 subhalos with numerically determined $M_{0.3}$ within the published $1-\sigma$ error bars and distances within 40% of the measured distance of the given dSph. The distances were calculated for 100 random observer locations 8kpc from the host halo center. We then determined the median value and the 16th and 84th percentiles of $(V_{\rm max}, r_{\rm Vmax})$ and $(V_{\rm peak}, r_{\rm Vpeak})$ of the subhalos associated with each dSph. These values are given in Table 1. The median values of $V_{\rm max}$ range from $5.0\,\text{km s}^{-1}$ (Leo IV) to $19\,\text{km s}^{-1}$ (Draco, Leo I), and of $V_{\rm peak}$ from $6.7\,\text{km s}^{-1}$ (Leo IV) to $30\,\text{km s}^{-1}$ (Ursa Minor, Carina). Note that, as expected, dSph's closer to the Galactic Center typically show a larger reduction from $V_{\rm peak}$ to $V_{\rm max}$, sometimes by more than a factor of 2.

In the same fashion, we then determine the most likely annihilation luminosities for the 18 dSph's by using (9) for an NFW profile to calculate the total luminosity $\mathcal{L}_{\rm tot}$ for every simulated subhalo. Additionally, we also determine $\mathcal{L}_{0.3}$, the luminosity within 0.3 kpc from the center, motivated by the fact that we only have dynamical evidence for a DM dominated potential out to this radius. Lastly we also consider two measures of the brightness of each halo: $\mathcal{F}_{\rm tot} = \mathcal{L}_{\rm tot}/4\pi D^2$, the total expected flux from the dSph, and $\mathcal{F}_c$, the flux from a central region subtending 0.15°, which is comparable to the angular resolution of *Fermi* above 3 GeV. $\mathcal{F}_c$ thus corresponds to the brightest "pixel" in a *Fermi* γ-ray image of a subhalo. These numbers are given in Table 2.

4.1. Current Observational Constraints. Several ACT have performed observations of a handful of dSph's.

(i) The H.E.S.S. array (consisting of four $107\,\text{m}^2$ telescopes with a 5° field of view and an energy threshold of 160 GeV [100]) has obtained an 11 hour exposure of the Sagittarius dwarf galaxy. No γ-ray signal was detected, resulting in a flux limit of $3.6 \times 10^{-12}\,\text{cm}^{-2}\,\text{s}^{-1}$ (95% confidence) at $E > 250\,\text{GeV}$, and a corresponding limit on the cross section of $\langle\sigma v\rangle \lesssim 10^{-23}\,\text{cm}^3\,\text{s}^{-1}$ for an NFW profile and $\langle\sigma v\rangle \lesssim 2 \times 10^{-25}\,\text{cm}^3\,\text{s}^{-1}$ for a cored profile (for a $m_\chi = 100\,\text{GeV} - 1\,\text{TeV}$ higgsino-type neutralino) [46]. Note that the Sagittarius dwarf is undergoing a strong tidal interaction with the Milky Way galaxy [101], and no confident determination of $M_{0.3}$ has been possible.

(ii) The VERITAS array (consisting of four $144\,\text{m}^2$ telescopes with a 3.5° field of view and an energy threshold of 100 GeV [102]) has conducted a 15 hours observation of Willman 1 and 20 hour observations each of Draco and Ursa Minor [47]. No γ-ray signal was detected at a flux limit of ~1% of the flux from the Crab Nebula, corresponding to a limit of $2.4 \times 10^{-12}\,\text{cm}^{-2}\,\text{s}^{-1}$ (95% confidence) at $E > 200\,\text{GeV}$ [103].

(iii) Additionally the MAGIC [48, 49] and STACEE [50] telescopes have reported observations of Willman 1 and Draco, resulting in comparable or slightly higher flux limits.

To convert the values of $\mathcal{F}_c$ in Table 2 into physical fluxes that can directly be compared to these observational limits, it would be necessary to obtain values of the particle

Table 1: The properties of likely DM subhalos of the 18 Milky Way dSph galaxies for which $M_{0.3}$ values (column 3) have been published [33]. $V_{\rm max}$ and $r_{\rm Vmax}$ are the maximum circular velocity and its radius, $V_{\rm peak}$ and $r_{\rm Vpeak}$ the largest $V_{\rm max}$ a subhalo ever acquired and its corresponding radius. The first number is the median over all *Via Lactea II* subhalos matching the dSph's distance and $M_{0.3}$, the numbers in parentheses the 16th and 84th percentiles (see text for details).

Name	D [kpc]	$M_{0.3}$ [$10^7\,M_\odot$]	$V_{\rm max}$ [km s^{-1}]	$r_{\rm Vmax}$ [kpc]	$V_{\rm peak}$ [km s^{-1}]	$r_{\rm Vpeak}$ [kpc]
Segue 1	23	$1.58^{+3.30}_{-1.11}$	$10\,\left(^{17}_{8.4}\right)$	$0.43\,\left(^{0.89}_{0.29}\right)$	$26\,\left(^{55}_{13}\right)$	$2.4\,\left(^{33}_{1.4}\right)$
Ursa Major II	32	$1.09^{+0.89}_{-0.44}$	$13\,\left(^{17}_{11}\right)$	$0.59\,\left(^{0.89}_{0.31}\right)$	$27\,\left(^{33}_{17}\right)$	$3.3\,\left(^{14}_{2.4}\right)$
Wilman 1	38	$0.77^{+0.89}_{-0.42}$	$8.3\,\left(^{11}_{7.5}\right)$	$0.38\,\left(^{0.62}_{0.29}\right)$	$15\,\left(^{27}_{10}\right)$	$2.0\,\left(^{3.9}_{0.90}\right)$
Coma Berenices	44	$0.72^{+0.36}_{-0.28}$	$9.1\,\left(^{12}_{8.2}\right)$	$0.42\,\left(^{0.62}_{0.31}\right)$	$15\,\left(^{25}_{11}\right)$	$1.9\,\left(^{3.4}_{0.97}\right)$
Ursa Minor	66	$1.79^{+0.37}_{-0.59}$	$18\,\left(^{21}_{15}\right)$	$0.81\,\left(^{1.8}_{0.61}\right)$	$30\,\left(^{56}_{21}\right)$	$3.8\,\left(^{9.7}_{2.8}\right)$
Draco	80	$1.87^{+0.20}_{-0.29}$	$19\,\left(^{22}_{17}\right)$	$0.86\,\left(^{2.4}_{0.81}\right)$	$28\,\left(^{37}_{26}\right)$	$3.8\,\left(^{32}_{2.4}\right)$
Sculptor	80	$1.20^{+0.11}_{-0.37}$	$13\,\left(^{15}_{12}\right)$	$0.64\,\left(^{1.0}_{0.54}\right)$	$20\,\left(^{25}_{16}\right)$	$2.9\,\left(^{5.6}_{1.6}\right)$
Sextans	86	$0.57^{+0.45}_{-0.14}$	$9.7\,\left(^{12}_{8.5}\right)$	$0.52\,\left(^{0.89}_{0.37}\right)$	$14\,\left(^{19}_{11}\right)$	$1.6\,\left(^{3.0}_{0.97}\right)$
Carina	101	$1.57^{+0.19}_{-0.10}$	$17\,\left(^{22}_{16}\right)$	$1.00\,\left(^{2.3}_{0.69}\right)$	$30\,\left(^{42}_{24}\right)$	$3.8\,\left(^{32}_{3.3}\right)$
Ursa Major I	106	$1.10^{+0.70}_{-0.29}$	$14\,\left(^{17}_{13}\right)$	$0.84\,\left(^{1.3}_{0.61}\right)$	$20\,\left(^{30}_{16}\right)$	$3.2\,\left(^{6.8}_{1.6}\right)$
Fornax	138	$1.14^{+0.09}_{-0.12}$	$15\,\left(^{16}_{14}\right)$	$1.1\,\left(^{1.3}_{0.64}\right)$	$20\,\left(^{24}_{18}\right)$	$3.0\,\left(^{6.1}_{1.9}\right)$
Hercules	138	$0.72^{+0.51}_{-0.21}$	$11\,\left(^{14}_{9.4}\right)$	$0.69\,\left(^{1.1}_{0.45}\right)$	$14\,\left(^{20}_{12}\right)$	$1.9\,\left(^{3.8}_{1.2}\right)$
Canes Venatici II	151	$0.70^{+0.53}_{-0.25}$	$11\,\left(^{13}_{8.9}\right)$	$0.67\,\left(^{1.1}_{0.44}\right)$	$14\,\left(^{19}_{11}\right)$	$1.8\,\left(^{3.7}_{1.1}\right)$
Leo IV	158	$0.39^{+0.50}_{-0.29}$	$5.0\,\left(^{7.2}_{4.2}\right)$	$0.35\,\left(^{0.57}_{0.22}\right)$	$6.7\,\left(^{10}_{5.0}\right)$	$0.84\,\left(^{1.7}_{0.48}\right)$
Leo II	205	$1.43^{+0.23}_{-0.15}$	$18\,\left(^{21}_{16}\right)$	$1.5\,\left(^{2.1}_{0.93}\right)$	$24\,\left(^{28}_{19}\right)$	$4.1\,\left(^{8.2}_{2.4}\right)$
Canes Venatici I	224	$1.40^{+0.18}_{-0.19}$	$18\,\left(^{20}_{16}\right)$	$1.5\,\left(^{2.1}_{1.0}\right)$	$22\,\left(^{29}_{18}\right)$	$2.9\,\left(^{6.1}_{2.1}\right)$
Leo I	250	$1.45^{+0.27}_{-0.20}$	$19\,\left(^{21}_{17}\right)$	$1.7\,\left(^{3.1}_{1.1}\right)$	$25\,\left(^{27}_{19}\right)$	$2.9\,\left(^{6.3}_{2.1}\right)$
Leo T	417	$1.30^{+0.88}_{-0.42}$	$16\,\left(^{21}_{13}\right)$	$1.2\,\left(^{2.4}_{0.85}\right)$	$19\,\left(^{26}_{17}\right)$	$2.4\,\left(^{6.1}_{1.6}\right)$

physics term of (7) by performing a scan of the DM model parameter space. This is beyond the scope of this work, but a similar analysis has been performed by others [83, 103–106]. Current ACT observations of dSph's are beginning to directly constrain DM models, and future longer exposure time observations of additional dSph's (in particular Segue 1 and Ursa Major II) with a lower threshold energy hold great potential. We also eagerly await the first *Fermi* data on fluxes from the known dSph galaxies.

5. Dark Clumps

An annihilation signal from dark clumps not associated with any known luminous stellar counterpart would provide evidence for one of the fundamental implications of the CDM paradigm of structure formation: abundant Galactic substructure. Barring a serendipitous discovery with an ACT, the discovery of such a source will have to rely on all-sky surveys, such as provided by *Fermi*. Of course even a weak and tentative identification of a dark clump with *Fermi* could be followed up with an ACT.

Unlike for known dSph galaxies, for which we at least have some astronomical observations to guide us, we must rely entirely upon numerical simulations to quantify the prospects of detecting the annihilation signal from dark clumps. Recent significant progress [107] notwithstanding, it is at present not yet possible to perform realistic cosmological hydrodynamic galaxy-formation simulations, which include, in addition to the DM dynamics, all the relevant baryonic physics of gas cooling, star formation, supernova and AGN feedback, and so forth. that may have a significant impact on the DM distribution at the centers of massive halos. Instead we make use of the extremely high resolution, purely collisionless DM-only *Via Lactea II* (VL2) simulation [13], which provides an exquisite view of the clumpiness

Table 2: Estimated luminosities and fluxes for the 18 dSph from Table 1. $\mathcal{L}_{\rm tot}$ is the total luminosity and $\mathcal{L}_{0.3}$ the luminosity from within the central 0.3 kpc. $\mathcal{F}_{\rm tot} = \mathcal{L}_{\rm tot}/4\pi D^2$ is the total flux and $\mathcal{F}_c$ the flux from a central region subtending 0.15° (about the angular resolution of *Fermi* above 3 GeV). The first number is the median over all subhalos matching the dSph distance and $M_{0.3}$, the numbers in parentheses are the 16th and 84th percentiles. The table is ordered by decreasing $\mathcal{F}_{\rm tot}$.

Name	D [kpc]	$\mathcal{L}_{\rm tot}$ [$10^6\,M_\odot^2\,pc^{-3}$]	$\mathcal{L}_{0.3}$ [$10^6\,M_\odot^2\,pc^{-3}$]	$\mathcal{F}_{\rm tot}$ [$10^{-5}\,M_\odot^2\,pc^{-5}$]	$\mathcal{F}_c$ [$10^{-5}\,M_\odot^2\,pc^{-5}$]
Segue 1	23	$2.8\,\binom{7.2}{0.93}$	$2.5\,\binom{6.1}{0.89}$	$41\,\binom{110}{14}$	$12\,\binom{34}{5.6}$
Ursa Major II	32	$3.5\,\binom{7.2}{2.8}$	$3.1\,\binom{6.1}{2.5}$	$28\,\binom{56}{21}$	$9.5\,\binom{18}{7.7}$
Ursa Minor	66	$6.2\,\binom{9.4}{5.1}$	$4.7\,\binom{7.3}{3.1}$	$11\,\binom{17}{9.3}$	$5.2\,\binom{8.4}{2.5}$
Draco	80	$7.0\,\binom{9.9}{6.0}$	$5.6\,\binom{8.2}{3.1}$	$8.8\,\binom{12}{7.4}$	$4.3\,\binom{6.4}{1.7}$
Carina	101	$7.0\,\binom{9.4}{4.8}$	$5.6\,\binom{7.3}{3.5}$	$5.5\,\binom{7.3}{3.7}$	$3.1\,\binom{3.8}{1.6}$
Wilman 1	38	$0.88\,\binom{2.9}{0.55}$	$0.85\,\binom{2.7}{0.53}$	$4.9\,\binom{16}{3.0}$	$2.6\,\binom{6.4}{1.5}$
Coma Berenices	44	$1.2\,\binom{2.8}{0.78}$	$1.1\,\binom{2.5}{0.70}$	$4.8\,\binom{11}{3.2}$	$2.5\,\binom{5.1}{1.6}$
Sculptor	80	$2.9\,\binom{3.7}{2.3}$	$2.5\,\binom{3.3}{2.0}$	$3.7\,\binom{4.6}{2.8}$	$2.0\,\binom{2.8}{1.6}$
Ursa Major I	106	$3.3\,\binom{5.4}{2.3}$	$2.5\,\binom{4.5}{1.9}$	$2.3\,\binom{3.8}{1.6}$	$1.3\,\binom{2.4}{0.91}$
Fornax	138	$3.5\,\binom{4.4}{3.0}$	$2.9\,\binom{3.3}{2.3}$	$1.4\,\binom{1.8}{1.3}$	$1.00\,\binom{1.2}{0.74}$
Sextans	86	$1.2\,\binom{2.0}{0.77}$	$1.1\,\binom{1.8}{0.69}$	$1.3\,\binom{2.1}{0.83}$	$0.86\,\binom{1.4}{0.55}$
Leo II	205	$4.6\,\binom{6.5}{3.8}$	$3.1\,\binom{4.7}{2.1}$	$0.88\,\binom{1.2}{0.73}$	$0.55\,\binom{0.85}{0.37}$
Canes Venatici I	224	$4.6\,\binom{7.9}{3.8}$	$3.1\,\binom{5.0}{2.3}$	$0.73\,\binom{1.3}{0.60}$	$0.48\,\binom{0.79}{0.35}$
Leo I	250	$5.2\,\binom{7.9}{3.9}$	$3.2\,\binom{5.4}{2.3}$	$0.66\,\binom{1.0}{0.50}$	$0.41\,\binom{0.73}{0.31}$
Hercules	138	$1.4\,\binom{2.6}{0.94}$	$1.2\,\binom{2.2}{0.80}$	$0.57\,\binom{1.1}{0.39}$	$0.42\,\binom{0.74}{0.28}$
Canes Venatici II	151	$1.2\,\binom{2.5}{0.79}$	$1.1\,\binom{2.0}{0.68}$	$0.44\,\binom{0.88}{0.27}$	$0.33\,\binom{0.59}{0.21}$
Leo T	417	$3.5\,\binom{8.2}{2.4}$	$2.2\,\binom{4.1}{1.7}$	$0.16\,\binom{0.38}{0.11}$	$0.12\,\binom{0.24}{0.093}$
Leo IV	158	$0.14\,\binom{0.43}{0.063}$	$0.13\,\binom{0.39}{0.060}$	$0.043\,\binom{0.14}{0.020}$	$0.039\,\binom{0.12}{0.018}$

of the Galactic DM distribution, but at the expense of not capturing all the relevant physics at the baryon-dominated Galactic center. For the abundance, distribution, and internal properties of the DM subhalos that are the focus of this work, the neglect of baryonic physics is less of a problem, since they are too small to allow for much gas cooling and significant baryonic effects (this is supported by the high mass-to-light ratios observed in the Milky Way dSph's), although tidal interactions with the Galactic stellar and gaseous disk might significantly affect the population of nearby subhalos.

With a particle mass of $4,100\,M_\odot$ and a force softening of 40 pc, the VL2 simulation resolves over 50,000 subhalos today within the host's $r_{200} = 402$ kpc (the radius enclosing an average density 200 times the mean matter value). Above ~200 particles per halo, the differential subhalo mass function is well-fit by a single power law, $dN/dM \sim M^{-1.9}$, and the cumulative $V_{\rm max}$ function is $N(>V_{\rm max}) \sim V_{\rm max}^{-3}$ [13]. The radial distribution of subhalos is "antibiased" with respect to the host halo's density profile, meaning that the mass distribution becomes less clumpy as one approaches the host's center [13, 90]. Similar results have been obtained by the Aquarius group [14, 88]. Typical subhalo concentrations, defined as $\Delta_V = \langle\rho(<r_{\rm Vmax})\rangle/\rho_{\rm crit}$, grow towards the center, owing to a combination of earlier formation times [108, 109] and stronger tidal stripping of central subhalos: VL2 subhalos on average have a 60 times higher Δ_V at 8 kpc than at 400 kpc [13]. Note that this also implies ~7 times higher annihilation luminosities for central subhalos, since $\mathcal{L} \sim V_{\rm max}^4/r_{\rm Vmax} \sim V_{\rm max}^3\sqrt{\Delta_V}$. The counter-acting trends of decreasing relative abundance of subhalos and increasing annihilation luminosity towards the center makes it more difficult for (semi-)analytical methods to accurately assess the role of subhalos in the Galactic annihilation signal, and motivate future, even higher resolution, numerical

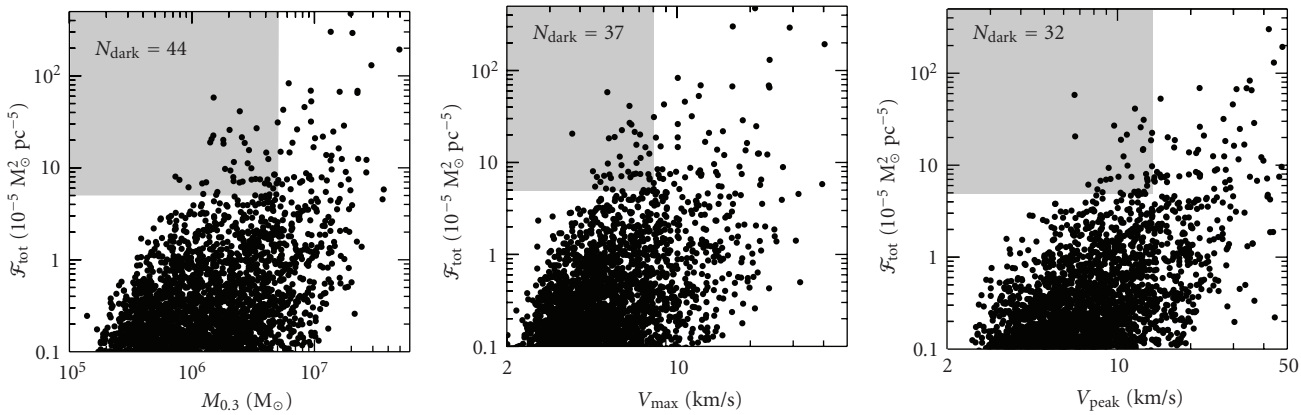

FIGURE 3: The annihilation flux $\mathcal{F}_{\rm tot}$ from subhalos in the *Via Lactea II* simulation versus their $M_{0.3}$, $V_{\rm max}$, and $V_{\rm peak}$. The gray shaded areas indicate regions containing subhalos with $\mathcal{F}_{\rm tot}$ as least as high as the fifth-brightest Milky Way dSph galaxy (Carina), but with $M_{0.3} < 5 \times 10^6\,M_\odot$, $V_{\rm max} < 8\,{\rm km\,s^{-1}}$, and $V_{\rm peak} < 14\,{\rm km\,s^{-1}}$, that is, probable dark clumps. Only one of the 100 random observer locations used in the analysis is shown here. The number $N_{\rm dark}$ in the top left refers to the number of "dark clumps" for this particular observer location.

simulations of the formation and evolution of Galactic DM (sub-)structure. A direct analysis of the VL2 simulations in terms of the detectability with *Fermi* of individual subhalos was performed by [82]. They found that for reasonable particle physics parameters a handful of subhalos should be able to outshine the astrophysical backgrounds and would be detected at more than 5σ significance over the lifetime of the *Fermi* mission.

As discussed in the previous section, we have directly calculated the annihilation luminosities for all VL2 subhalos using (9) and assuming an NFW density profile. The luminosities would be ∼40% *higher* if an Einasto ($\alpha = 0.17$) profile had been adopted instead. We then converted these luminosities to fluxes by dividing by $4\pi D^2$, where the distances D were determined for 100 randomly chosen observer locations 8 kpc from the host halo center. The resulting values of $\mathcal{F}_{\rm tot}$ are plotted in Figure 3, for just one of the 100 observer positions, as a function of the subhalos' $M_{0.3}$, $V_{\rm max}$, and $V_{\rm peak}$. Although the distributions show quite a bit of scatter, in all three cases a clear trend is apparent of more massive subhalos having higher fluxes. This trend could simply be the result of the higher luminosities of more massive halos, but one might have expected smaller mass subhalos to be brighter, since their greater abundance should result in lower typical distances and hence higher fluxes. This latter effect could be artificially suppressed in the numerical simulations, if smaller mass subhalos, whose dense centers are not as well resolved, were more easily tidally disrupted closer to the Galactic Center, or if the subhalo finding algorithm had trouble identifying low mass halos in the high background density central region. In Figure 4 we plot the subhalos' $V_{\rm max}$ against their distance to the host halo center $\hat{D}$. There appears to be a dearth of the lowest $V_{\rm max}$ subhalos ($V_{\rm max} \lesssim 2\,{\rm km\,s^{-1}}$) at small distances, but at the moment it is not clear whether this suppression is a real effect or a numerical artifact. It is also worth noting that such small subhalos might be more susceptible to disruption by

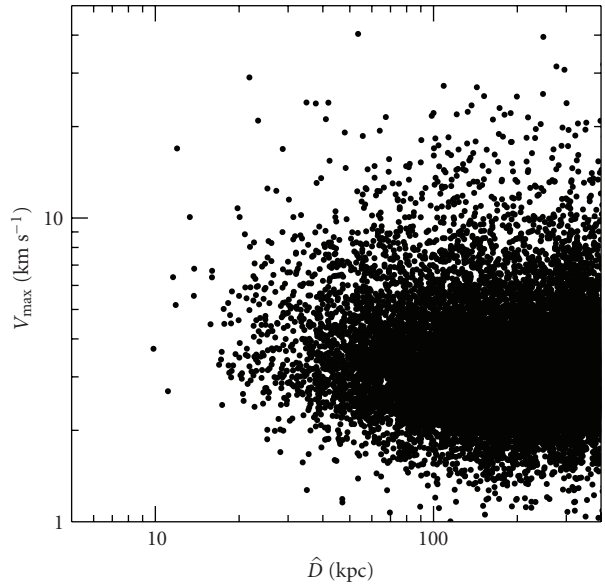

FIGURE 4: VL2 subhalo $V_{\rm max}$ versus distance to host halo $\hat{D}$.

interactions with the Milky Way's stellar and gaseous disk. At any rate, we can obtain an analytic estimate of the scaling of the typical subhalo flux with $V_{\rm max}$ by noting that the luminosity scales as $\mathcal{L} \sim V_{\rm max}^3\sqrt{\Delta_V}$ and the typical distance as $D \sim n^{-1/3} \sim V_{\rm max}^{4/3}$ (since $dn/dV_{\rm max} \sim V_{\rm max}^{-4}$). The typical flux should thus scale as $\mathcal{F} \sim \mathcal{L}/D^2 \sim V_{\rm max}^{1/3}\sqrt{\Delta_V}$, and would be higher for more massive subhalos at a fixed Δ_V. Actually lower $V_{\rm max}$ subhalos might be expected to have higher Δ_V due to their earlier formation times, but it remains to be seen to what degree this expectation is borne out in numerical simulations.

The points in Figure 3 can be directly compared with the values for the known Milky Way dSph's in Tables 1 and 2:

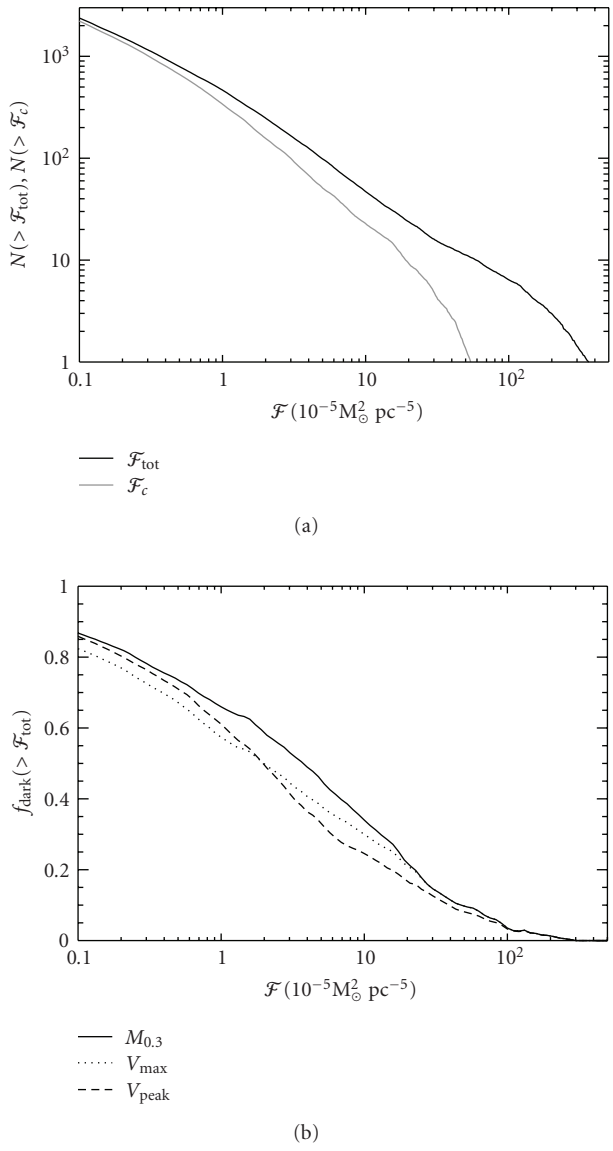

FIGURE 5: (a) The cumulative number of subhalos with flux exceeding $\mathcal{F}_{\rm tot}$, $\mathcal{F}_c$. (b) The fraction of dark clumps, that is, subhalos likely not hosting any stars and defined by $M_{0.3} < 5 \times 10^6\,\mathrm{M}_\odot$, $V_{\rm max} < 8\,\mathrm{km\,s^{-1}}$, or $V_{\rm peak} < 14\,\mathrm{km\,s^{-1}}$, as a function of limiting flux $\mathcal{F}_{\rm tot}$. These distributions are averages over 100 randomly chosen observer locations 8 kpc from the host halo center.

it appears that there are many DM subhalos at least as bright as the known Milky Way dSph's. This impression is confirmed by the top panel of Figure 5, in which we show the cumulative number of subhalos with fluxes greater than $\mathcal{F}_{\rm tot}$ and $\mathcal{F}_c$. These distributions were obtained by averaging over 100 randomly chosen observer locations 8 kpc from the host halo center. The mean number of DM subhalos with $\mathcal{F}_{\rm tot}$ greater than that of (Carina, Draco, Ursa Minor, Ursa Major, Segue 1) is $(90^{+4}_{-5}, 54^{+3}_{-3}, 43^{+3}_{-3}, 17^{+1}_{-1}, 13^{+1}_{-1})$ where the sub- and superscripts refer to the 16th and 84th percentile. The corresponding numbers for $\mathcal{F}_c$ are $(96^{+4}_{-6}, 62^{+5}_{-4}, 49^{+3}_{-2}, 24^{+2}_{-3}, 19^{+3}_{-3})$. This demonstrates that if a DM annihilation signal from any of the known Milky Way dSph's is detected, then many more DM subhalos should be visible. The plot also implies that Segue 1, the dSph with the highest $\mathcal{F}_{\rm tot}$ and $\mathcal{F}_c$ of the currently known sample, is unlikely to be the brightest DM subhalo in the sky. Of course some of these additional bright sources could very well have stellar counterparts that have simply been missed so far, due to the limited sky coverage of current surveys or insufficiently deep exposures. To assess what fraction of high flux sources are likely to be genuinely dark clumps without any stars, we split the sample by a limiting value of $M_{0.3} = 5 \times 10^6\,\mathrm{M}_\odot$, $V_{\rm max} = 8\,\mathrm{km\,s^{-1}}$, and $V_{\rm peak} = 14\,\mathrm{km\,s^{-1}}$. We assume that DM subhalos below these limits are too small to have been able to form any stars, and hence are truly dark clumps. Of the known dSph's listed in Table 1 only Leo IV falls below these limits. In the bottom panel of Figure 5 we plot $f_{\rm dark}(>\mathcal{F}_{\rm tot})$, the fraction of subhalos without stars, as a function of the limiting annihilation flux $\mathcal{F}_{\rm tot}$. $f_{\rm dark}$ falls monotonically with $\mathcal{F}_{\rm tot}$, which makes sense given that higher flux sources are typically more massive and hence more likely to host stars. Between 30% and 40% of all DM subhalos brighter than Carina are expected to be dark clumps. This fraction drops to 10% for subhalos brighter than Segue 1.

5.1. Boost Factor? The analysis presented here so far has been limited to known dSph galaxies and clumps resolved in the VL2 simulation, whose resolution limit is set by the available computational resources, and has nothing to do with fundamental physics. Indeed, the CDM expectation is that the clumpiness should continue all the way down to the cutoff in the matter power spectrum, set by collisional damping and free streaming in the early universe Green2005, Loeb2005. For typical WIMP DM, this cutoff occurs at masses of $m_0 = 10^{-12}$ to $10^{-4}\,\mathrm{M}_\odot$ [27, 28], some 10 to 20 orders of magnitude below VL2's mass resolution. Since the annihilation rate goes as ρ^2 and $\langle\rho^2\rangle > \langle\rho\rangle^2$, this sub-resolution clumpiness will lead to an enhancement of the total luminosity compared to the smooth mass distribution in the simulation.

The magnitude of this so-called substructure boost factor depends sensitively on the properties of subhalos below the simulation's resolution limit, in particular on the behavior of the concentration-mass relation. A simple power law extrapolation of the contribution of simulated subhalos to the total luminosity of the host halo leads to boosts on order of a a few hundred [55]. More sophisticated (semi-)analytical models, accounting for different possible continuations of the concentration-mass relation to lower masses, typically find smaller boosts of around a few tens [81, 82, 105, 110].

More importantly, this boost refers to the enhancement of the *total* annihilation luminosity of a subhalo, but this is not likely the quantity most relevant for detection. At the distances where subhalos might be detectable as individual sources, their projected size exceeds the angular resolution of today's detectors. The surface brightness profile from annihilations in the smooth DM component would be strongly peaked towards the center (yet probably still resolved by *Fermi* [82]), owing to the $\rho(r)^2$ dependence

of the annihilation rate. The luminosity contribution from a subhalo's sub-substructure population (i.e., its boost), however, is much less centrally concentrated: at best it follows the subhalo mass density profile $\rho(r)$, although it might very well even be antibiased. This implies that substructure would preferentially boost the outer regions of a subhalo, where the surface brightness typically remains below the level of astrophysical backgrounds and hence does not contribute much to the detection significance. In other words, the boost factor might apply to $\mathcal{F}_{\rm tot}$, but much less (or not at all) to $\mathcal{F}_c$; yet it is $\mathcal{F}_c$ that is likely to determine whether a given subhalo can be detected with *Fermi* or an ACT. It thus seems unlikely that the detectability of Galactic subhalos would be significantly enhanced by their own substructure. (This is in contrast to many previous claims in the literature, including some by the present author (e.g., [82]). A re-analysis of that work (in progress) with an improved treatment of the angular dependence of the substructure boost, indeed finds that the boost only weakly increases the number of detectable subhalos.) On the other hand, a substructure boost could be very important for diffuse DM annihilation signals, either from extragalactic sources, where the boost would simply increase the overall amplitude [111], or from Galactic DM, where the boost could affect the amplitude and angular profile of the signal, as well as the power spectrum of its anisotropies [51–53, 55, 81, 82].

Note also that local substructure boost factors of up to several hundreds, which have been invoked to explain the PAMELA satellite's measurement of an anomalously rising positron fraction at energies above 10 GeV as a DM annihilation signal, appear to be inconsistent with the results from high resolution numerical simulations like VL2 and Aquarius.

6. Summary and Conclusions

In this work we have reviewed the DM annihilation signal from Galactic subhalos. After going over the basics of the annihilation process with a focus on the resulting γ-ray output, we summarized the properties of DM subhalos relevant for estimating their annihilation luminosity. In the remainder of the paper we used the *Via Lactea II* simulation to assess the strength of the annihilation flux from both known Galactic dSph galaxies as well as from dark clumps not hosting any stars. By matching the distances D and central masses $M_{0.3}$ of simulated subhalos to the corresponding published values of 18 known dSph's, we were able to infer most probable values, and the 1-σ scatter around them, for $V_{\rm max}$ and $r_{\rm Vmax}$, and hence for the annihilation luminosity $\mathcal{L}$ and flux $\mathcal{F}$ of all dwarfs. According to this analysis, the recently discovered dSph Segue 1 should be the brightest of the known dSph's, followed by Ursa Major II, Ursa Minor, Draco, and Carina. Further, we showed that if any of the known Galactic dSph's are bright enough to be detected, then at least 10 times more subhalos should appear as visible sources. Some of these would be as-of-yet undiscovered luminous dwarf galaxies, but a significant fraction should correspond to dark clumps not hosting any stars. The fraction of dark clump sources is 10% for subhalos at least as bright as Segue 1 and grows to 40% for subhalos brighter than Carina. Lastly, we briefly considered the role that a substructure boost factor should play in the detectability of individual Galactic dSph's and other DM subhalos. We argued that any boost is unlikely to strongly increase their prospects for detection, since its shallower angular dependence would preferentially boost the outer regions of subhalos, which typically do not contribute much to the detection significance.

Several caveats to these findings are in order. Probably the most important of these is that our simulation completely neglects the effects of baryons. Gas cooling, star formation, and the associated feedback processes are unlikely to strongly affect most subhalos, owing to their low masses. However, tidal interactions with the baryonic components of the Milky Way galaxy might do so. The Sagittarius dSph, for example, is thought to be in the process of complete disruption from tidal interactions with the Milky Way. A second caveat is that our analysis is based on only one, albeit very high resolution, numerical simulation, and so we cannot assess the importance of cosmic variance, or the dependence on cosmological parameters such as σ_8 and n_s. Other work has found considerable halo-to-halo scatter [14, 112, 113], with a factor of $\sim$2 variance in the total subhalo abundance, for example.

These caveats motivate further study and future, higher resolution numerical simulations, including the effects of baryonic physics. The characterization of the Galactic DM annihilation signal is of crucial importance in guiding observational efforts to shed light on the nature of DM. We are hopeful that in the next few years the promise of a DM annihilation signal will come to fruition, and will help us to unravel this puzzle.

Acknowledgments

Support for this work was provided by the William L. Loughlin membership at the Institute for Advanced Study. The author would like to thank his collaborators from the Via Lactea Project for their expertise and invaluable contributions.

References

[1] A. Klypin, A. V. Kravtsov, O. Valenzuela, and F. Prada, "Where are the missing galactic satellites?" *Astrophysical Journal*, vol. 522, no. 1, part 1, pp. 82–92, 1999.

[2] B. Moore, S. Ghigna, F. Governato, et al., "Dark matter substructure within galactic halos," *Astrophysical Journal*, vol. 524, no. 1, part 2, pp. L19–L22, 1999.

[3] M. Mateo, "Dwarf galaxies of the local group," *Annual Review of Astronomy and Astrophysics*, vol. 36, pp. 435–506, 1998.

[4] B. Willman, M. R. Blanton, A. A. West, et al., "A new Milky Way companion: unusual globular cluster or extreme dwarf satellite?" *Astronomical Journal*, vol. 129, no. 6, pp. 2692–2700, 2005.

[5] B. Willman, J. J. Dalcanton, D. Martinez-Delgado, et al., "A new Milky Way dwarf galaxy in URSA Major," *Astrophysical Journal*, vol. 626, no. 2, part 2, pp. L85–L88, 2005.

[6] V. Belokurov, D. B. Zucker, N. W. Evans, et al., "The field of streams: sagittarius and its siblings," *Astrophysical Journal*, vol. 642, no. 2, part 2, pp. L137–L140, 2006.

[7] D. B. Zucker, V. Belokurov, N. W. Evans, et al., "A new Milky Way dwarf satellite in canes venatici," *Astrophysical Journal*, vol. 643, no. 2, part 2, pp. L103–L106, 2006.

[8] D. B. Zucker, V. Belokurov, N. W. Evans, et al., "A curious Milky Way satellite in Ursa Major," *Astrophysical Journal*, vol. 650, no. 1, part 2, pp. L41–L44, 2006.

[9] T. Sakamoto and T. Hasegawa, "Discovery of a faint old stellar system at 150 kpc," *Astrophysical Journal*, vol. 653, no. 1, part 2, pp. L29–L32, 2006.

[10] V. Belokurov, D. B. Zucker, N. W. Evans, et al., "Cats and dogs, hair and a hero: a quintet of new Milky Way companions," *Astrophysical Journal*, vol. 654, no. 2, part 1, pp. 897–906, 2007.

[11] M. J. Irwin, V. Belokurov, N. W. Evans, et al., "Discovery of an unusual dwarf galaxy in the outskirts of the Milky Way," *Astrophysical Journal*, vol. 656, no. 1, part 2, pp. L13–L16, 2007.

[12] S. M. Walsh, H. Jerjen, and B. Willman, "A pair of boötes: a new Milky Way satellite," *Astrophysical Journal*, vol. 662, no. 2, part 2, pp. L83–L86, 2007.

[13] J. Diemand, M. Kuhlen, P. Madau, et al., "Clumps and streams in the local dark matter distribution," *Nature*, vol. 454, no. 7205, pp. 735–738, 2008.

[14] V. Springel, J. Wang, M. Vogelsberger, et al., "The Aquarius Project: the subhaloes of galactic haloes," *Monthly Notices of the Royal Astronomical Society*, vol. 391, no. 4, pp. 1685–1711, 2008.

[15] J. Stadel, D. Potter, B. Moore, et al., "Quantifying the heart of darkness with GHALO—a multibillion particle simulation of a galactic halo," *Monthly Notices of the Royal Astronomical Society*, vol. 398, no. 1, pp. L21–L25, 2009.

[16] S. D. M. White and M. J. Rees, "Core condensation in heavy halos—a two-stage theory for galaxy formation and clustering," *Monthly Notices of the Royal Astronomical Society*, vol. 183, pp. 341–358, 1978.

[17] G. R. Blumenthal, S. M. Faber, J. R. Primack, and M. J. Rees, "Formation of galaxies and large-scale structure with cold dark matter," *Nature*, vol. 311, no. 5986, pp. 517–525, 1984.

[18] A. Dekel and J. Silk, "The origin of dwarf galaxies, cold dark matter, and biased galaxy formation," *Astrophysical Journal*, vol. 303, pp. 39–55, 1986.

[19] J. S. Bullock, A. V. Kravtsov, and D. H. Weinberg, "Reionization and the abundance of galactic satellites," *Astrophysical Journal*, vol. 539, no. 2, part 1, pp. 517–521, 2000.

[20] A. V. Kravtsov, O. Y. Gnedin, and A. A. Klypin, "The tumultuous lives of galactic dwarfs and the missing satellites problem," *Astrophysical Journal*, vol. 609, no. 2, part 1, pp. 482–497, 2004.

[21] L. Mayer, C. Mastropietro, J. Wadsley, J. Stadel, and B. Moore, "Simultaneous ram pressure and tidal stripping; how dwarf spheroidals lost their gas," *Monthly Notices of the Royal Astronomical Society*, vol. 369, no. 3, pp. 1021–1038, 2006.

[22] P. Madau, J. Diemand, and M. Kuhlen, "Dark matter subhalos and the dwarf satellites of the Milky Way," *Astrophysical Journal*, vol. 679, no. 2, pp. 1260–1271, 2008.

[23] S. E. Koposov, J. Yoo, H.-W. Rix, D. H. Weinberg, A. V. Macciò, and J. M. Escudé, "A quantitative explanation of the observed population of Milky Way satellite galaxies," *Astrophysical Journal*, vol. 696, pp. 2179–2194, 2009.

[24] A. V. Maccio', X. Kang, F. Fontanot, R. S. Somerville, S. E. Koposov, and P. Monaco, "On the origin and properties of Ultrafaint Milky Way Satellites in a LCDM Universe," submitted, http://arxiv.org/abs/0903.4681.

[25] A. M. Green, S. Hofmann, and D. J. Schwarz, "The first WIMPy halos," *Journal of Cosmology and Astroparticle Physics*, vol. 2005, no. 8, article 3, pp. 41–71, 2005.

[26] A. Loeb and M. Zaldarriaga, "Small-scale power spectrum of cold dark matter," *Physical Review D*, vol. 71, no. 10, Article ID 103520, 7 pages, 2005.

[27] S. Profumo, K. Sigurdson, and M. Kamionkowski, "What mass are the smallest protohalos?" *Physical Review Letters*, vol. 97, no. 3, Article ID 031301, 4 pages, 2006.

[28] T. Bringmann, "Particle models and the small-scale structure of dark matter," *New Journal of Physics*, vol. 11, no. 10, Article ID 105027, 105027 pages, 2009.

[29] E. W. Kolb and I. I. Tkachev, "Femtolensing and picolensing by axion miniclusters," *Astrophysical Journal*, vol. 460, no. 1, part 2, pp. L25–L28, 1996.

[30] C. Schmid, D. J. Schwarz, and P. Widerin, "Amplification of cosmological inhomogeneities by the QCD transition," *Physical Review D*, vol. 59, no. 4, Article ID 043517, 20 pages, 1999.

[31] P. Sikivie, "Axion cosmology," in *Axions: Theory, Cosmology, and Experimental Searches*, M. Kuster, G. Raffelt, and B. Beltrán, Eds., vol. 741 of *Lecture Notes in Physics*, p. 19, Springer, Berlin, Germany, 2008.

[32] L. Bergström, J. Edsjö, P. Gondolo, and P. Ullio, "Clumpy neutralino dark matter," *Physical Review D*, vol. 59, no. 4, Article ID 043506, 11 pages, 1999.

[33] L. E. Strigari, J. S. Bullock, M. Kaplinghat, et al., "A common mass scale for satellite galaxies of the Milky Way," *Nature*, vol. 454, no. 7208, pp. 1096–1097, 2008.

[34] R. A. Ibata, G. F. Lewis, M. J. Irwin, and T. Quinn, "Uncovering cold dark matter halo substructure with tidal streams," *Monthly Notices of the Royal Astronomical Society*, vol. 332, no. 4, pp. 915–920, 2002.

[35] K. V. Johnston, D. N. Spergel, and C. Haydn, "How lumpy is the Milky Way's dark matter halo?" *Astrophysical Journal*, vol. 570, no. 2, part 1, pp. 656–664, 2002.

[36] J. Peñarrubia, A. J. Benson, D. Martínez-Delgado, and H. W. Rix, "Modeling tidal streams in evolving dark matter halos," *Astrophysical Journal*, vol. 645, no. 1, part 1, pp. 240–255, 2006.

[37] J. M. Siegal-Gaskins and M. Valluri, "Signatures of ΛCDM substructure in tidal debris," *Astrophysical Journal*, vol. 681, no. 1, pp. 40–52, 2008.

[38] G. Toth and J. P. Ostriker, "Galactic disks, infall, and the global value of Ω," *Astrophysical Journal*, vol. 389, no. 1, pp. 5–26, 1992.

[39] J. I. Read, G. Lake, O. Agertz, and V. P. Debattista, "Thin, thick and dark discs in ΛCDM," *Monthly Notices of the Royal Astronomical Society*, vol. 389, no. 3, pp. 1041–1057, 2008.

[40] S. Kazantzidis, A. R. Zentner, A. V. Kravtsov, J. S. Bullock, and V. P. Debattista, "Cold dark matter substructure and galactic disks. II. Dynamical effects of hierarchical satellite accretion," *Astrophysical Journal*, vol. 700, no. 2, pp. 1896–1920, 2009.

[41] O. Adriani, G. C. Barbarino, G. A. Bazilevskaya, et al., "An anomalous positron abundance in cosmic rays with energies 1.5–100 GeV," *Nature*, vol. 458, no. 7238, pp. 607–609, 2009.

[42] J. Chang, J. H. Adams Jr., H. S. Ahn, et al., "An excess of cosmic ray electrons at energies of 300–800 GeV," *Nature*, vol. 456, no. 7220, pp. 362–365, 2008.

[43] S. Torii, T. Yamagami, T. Tamura, et al., "High-energy electron observations by PPB-BETS flight in Antarctica," submitted, http://arxiv.org/abs/0809.0760.

[44] A. A. Abdo, M. Ackermann, M. Ajello, et al., "Measurement of the cosmic ray $e^+ + e^-$ spectrum from 20 GeV to 1 TeV with the fermi large area telescope," *Physical Review Letters*, vol. 102, no. 18, Article ID 181101, 2009.

[45] F. Aharonian, A. G. Akhperjanian, G. Anton, et al., "Probing the ATIC peak in the cosmic-ray electron spectrum with H.E.S.S," submitted, http://arxiv.org/abs/0905.0105.

[46] F. Aharonian, A. G. Akhperjanian, A. R. Bazer-Bachi, et al., "Observations of the Sagittarius dwarf galaxy by the HESS experiment and search for a dark matter signal," *Astroparticle Physics*, vol. 29, no. 1, pp. 55–62, 2008.

[47] C. M. Hui, "VERITAS Observations of Extragalactic Non-Blazars," in *High Energy Gamma-Ray Astronomy: Proceedings of the 4th International Meeting on High Energy Gamma-Ray Astronomy*, F. A. Aharonian, W. Hofmann, and F. Rieger, Eds., vol. 1085 of *American Institute of Physics Conference Series*, pp. 407–410, 2008.

[48] J. Albert, E. Aliu, H. Anderhub, et al., "Upper limit for γ-ray emission above 140 GeV from the dwarf spheroidal galaxy draco," *Astrophysical Journal*, vol. 679, no. 1, pp. 428–431, 2008.

[49] E. Aliu, H. Anderhub, L. A. Antonelli, et al., "Upper limits on the vhe gamma-ray emission from the willman 1 satellite galaxy with the magic telescope," *Astrophysical Journal*, vol. 697, no. 2, pp. 1299–1304, 2009.

[50] D. D. Driscoll, C. E. Covault, J. Ball, et al., "Search for dark matter annihilation in Draco with the Solar Tower Atmospheric Cherenkov Effect Experiment," *Physical Review D*, vol. 78, no. 8, Article ID 087101, 4 pages, 2008.

[51] J. M. Siegal-Gaskins, "Revealing dark matter substructure with anisotropies in the diffuse gamma-ray background," *Journal of Cosmology and Astroparticle Physics*, vol. 2008, no. 10, article 40, 2008.

[52] S. Ando, "Gamma-ray background anisotropy from Galactic dark matter substructure," *Physical Review D*, vol. 80, no. 2, Article ID 023520, 16 pages, 2009.

[53] M. Fornasa, L. Pieri, G. Bertone, and E. Branchini, "Anisotropy probe of galactic and extra-galactic dark matter annihilations," *Physical Review D*, vol. 80, no. 2, Article ID 023518, 2009.

[54] F. Stoehr, S. D. M. White, V. Springel, G. Tormen, and N. Yoshida, "Dark matter annihilation in the halo of the Milky Way," *Monthly Notices of the Royal Astronomical Society*, vol. 345, no. 4, pp. 1313–1322, 2003.

[55] V. Springel, S. D. M. White, C. S. Frenk, et al., "Prospects for detecting supersymmetric dark matter in the Galactic halo," *Nature*, vol. 456, no. 7218, pp. 73–76, 2008.

[56] P. Brun, T. Delahaye, J. Diemand, S. Profumo, and P. Salati, "Cosmic ray lepton puzzle in the light of cosmological N-body simulations," *Physical Review D*, vol. 80, no. 3, Article ID 035023, 5 pages, 2009.

[57] M. Kuhlen and D. Malyshev, "ATIC, PAMELA, HESS, and Fermi data and nearby dark matter subhalos," *Physical Review D*, vol. 79, no. 12, Article ID 123517, 12 pages, 2009.

[58] N. Arkani-Hamed, D. P. Finkbeiner, T. R. Slatyer, and N. Weiner, "A theory of dark matter," *Physical Review D*, vol. 79, no. 1, Article ID 015014, 16 pages, 2009.

[59] M. Lattanzi and J. Silk, "Can the WIMP annihilation boost factor be boosted by the Sommerfeld enhancement?" *Physical Review D*, vol. 79, no. 8, Article ID 083523, 8 pages, 2009.

[60] L. Pieri, M. Lattanzi, and J. Silk, "Constraining the dark matter annihilation cross-section with Cherenkov telescope observations of dwarf galaxies," *Monthly Notices of the Royal Astronomical Society*, vol. 399, no. 4, pp. 2033–2040, 2009.

[61] M. Kuhlen, P. Madau, and J. Silk, "Exploring dark matter with milky way substructure," *Science*, vol. 325, no. 5943, pp. 970–973, 2009.

[62] M. S. Turner, "Windows on the axion," *Physics Report*, vol. 197, no. 2, pp. 67–97, 1990.

[63] E. W. Kolb and M. S. Turner, "The early universe," in *Frontiers in Physics*, Addison-Wesley, Reading, Mass, USA, 1990.

[64] G. Jungman, M. Kamionkowski, and K. Griest, "Supersymmetric dark matter," *Physics Report*, vol. 267, no. 5-6, pp. 195–373, 1996.

[65] G. Bertone, D. Hooper, and J. Silk, "Particle dark matter: evidence, candidates and constraints," *Physics Reports*, vol. 405, no. 5-6, pp. 279–390, 2005.

[66] G. Hinshaw, J. L. Weiland, R. S. Hill, et al., "Five-year wilkinson microwave anisotropy probe observations: data processing, sky maps and basic results," *Astrophysical Journal*, vol. 180, no. 2, pp. 225–245, 2009.

[67] K. Griest and D. Seckel, "Three exceptions in the calculation of relic abundances," *Physical Review D*, vol. 43, no. 10, pp. 3191–3203, 1991.

[68] P. Gondolo and G. Gelmini, "Cosmic abundances of stable particles: improved analysis," *Nuclear Physics B*, vol. 360, no. 1, pp. 145–179, 1991.

[69] T. Bringmann, L. Bergström, and J. Edsjö, "New gamma-ray contributions to supersymmetric dark matter annihilation," *Journal of High Energy Physics*, vol. 2008, no. 1, p. 49, 2008.

[70] M. Gustafsson, E. Lundström, L. Bergström, and J. Edsjö, "Significant gamma lines from inert higgs dark matter," *Physical Review Letters*, vol. 99, no. 4, Article ID 041301, 4 pages, 2007.

[71] T. Sjöstrand, "High-energy-physics event generation with PYTHIA 5.7 and JETSET 7.4," *Computer Physics Communications*, vol. 82, no. 1, pp. 74–89, 1994.

[72] P. Gondolo, J. Edsjö, P. Ullio, L. Bergström, M. Schelke, and E. A. Baltz, "DarkSUSY: computing supersymmetric dark matter properties numerically," *Journal of Cosmology and Astroparticle Physics*, vol. 2004, no. 7, article 8, pp. 145–179, 2004.

[73] C. Calcáneo-Roldán and B. Moore, "Surface brightness of dark matter: unique signatures of neutralino annihilation in the galactic halo," *Physical Review D*, vol. 62, no. 12, Article ID 123005, 10 pages, 2000.

[74] E. A. Baltz, C. Briot, P. Salati, R. Taillet, and J. Silk, "Detection of neutralino annihilation photons from external galaxies," *Physical Review D*, vol. 61, no. 2, Article ID 023514, 10 pages, 2000.

[75] A. Tasitsiomi and A. V. Olinto, "Detectability of neutralino clumps via atmospheric Cherenkov telescopes," *Physical Review D*, vol. 66, no. 8, Article ID 083006, 16 pages, 2002.

[76] R. Aloisio, P. Blasi, and A. V. Olinto, "Gamma-ray constraints on neutralino dark matter clumps in the galactic halo," *Astrophysical Journal*, vol. 601, no. 1, part 1, pp. 47–53, 2004.

[77] N. W. Evans, F. Ferrer, and S. Sarkar, "A travel guide to the dark matter annihilation signal," *Physical Review D*, vol. 69, no. 12, Article ID 123501, 10 pages, 2004.

[78] S. M. Koushiappas, A. R. Zentner, and T. P. Walker, "Observability of gamma rays from neutralino annihilations in the Milky Way substructure," *Physical Review D*, vol. 69, no. 4, Article ID 043501, 11 pages, 2004.

[79] S. M. Koushiappas, "Proper motion of gamma rays from microhalo sources," *Physical Review Letters*, vol. 97, no. 19, Article ID 191301, 4 pages, 2006.

[80] J. Diemand, M. Kuhlen, and P. Madau, "Dark matter substructure and gamma-ray annihilation in the Milky Way halo," *Astrophysical Journal*, vol. 657, no. 1, part 1, pp. 262–270, 2007.

[81] L. Pieri, G. Bertone, and E. Branchini, "Dark matter annihilation in substructures revised," *Monthly Notices of the Royal Astronomical Society*, vol. 384, no. 4, pp. 1627–1637, 2008.

[82] M. Kuhlen, J. Diemand, and P. Madau, "The dark matter annihilation signal from galactic substructure: predictions for glast," *Astrophysical Journal*, vol. 686, no. 1, pp. 262–278, 2008.

[83] L. E. Strigari, S. M. Koushiappas, J. S. Bullock, et al., "The most dark-matter-dominated galaxies: predicted gamma-ray signals from the faintest Milky Way dwarfs," *Astrophysical Journal*, vol. 678, no. 2, pp. 614–620, 2008.

[84] E. A. Baltz, J. E. Taylor, and L. L. Wai, "Can astrophysical gamma-ray sources mimic dark matter annihilation in galactic satellites?" *Astrophysical Journal*, vol. 659, no. 2, part 2, pp. L125–L128, 2007.

[85] J. F. Navarro, C. S. Frenk, and S. D. M. White, "A universal density profile from hierarchical clustering," *Astrophysical Journal*, vol. 490, no. 2, part 1, pp. 493–508, 1997.

[86] A. V. Macciò, A. A. Dutton, F. C. van den Bosch, B. Moore, D. Potter, and J. Stadel, "Concentration, spin and shape of dark matter haloes: scatter and the dependence on mass and environment," *Monthly Notices of the Royal Astronomical Society*, vol. 378, no. 1, pp. 55–71, 2007.

[87] J. Diemand, B. Moore, and J. Stadel, "Convergence and scatter of cluster density profiles," *Monthly Notices of the Royal Astronomical Society*, vol. 353, no. 2, pp. 624–632, 2004.

[88] J. F. Navarro, A. Ludlow, V. Springel, et al., "The diversity and similarity of simulated cold dark matter halos," submitted, http://arxiv.org/abs/0810.1522.

[89] B. Allgood, R. A. Flores, J. R. Primack, et al., "The shape of dark matter haloes: dependence on mass, redshift, radius and formation," *Monthly Notices of the Royal Astronomical Society*, vol. 367, no. 4, pp. 1781–1796, 2006.

[90] M. Kuhlen, J. Diemand, and P. Madau, "The shapes, orientation, and alignment of galactic dark matter subhalos," *Astrophysical Journal*, vol. 671, no. 2, pp. 1135–1146, 2007.

[91] G. L. Bryan and M. L. Norman, "Statistical properties of X-ray clusters: analytic and numerical comparisons," *Astrophysical Journal*, vol. 495, no. 1, part 1, pp. 80–99, 1998.

[92] J. T. Kleyna, M. I. Wilkinson, N. Evans, and G. Gilmore, "Ursa Major: a missing low-mass CDM halo?" *Astrophysical Journal*, vol. 630, no. 2, part 2, pp. L141–L144, 2005.

[93] R. R. Muñoz, J. L. Carlin, P. M. Frinchaboy, D. L. Nidever, S. R. Majewski, and R. J. Patterson, "Exploring halo substructure with giant stars: the dynamics and metallicity of the dwarf spheroidal in Boötes," *Astrophysical Journal*, vol. 650, no. 1, part 2, pp. L51–L54, 2006.

[94] N. F. Martin, R. A. Ibata, S. C. Chapman, M. Irwin, and G. F. Lewis, "A Keck/DEIMOS spectroscopic survey of faint Galactic satellites: searching for the least massive dwarf galaxies," *Monthly Notices of the Royal Astronomical Society*, vol. 380, no. 1, pp. 281–300, 2007.

[95] J. D. Simon and M. Geha, "The kinematics of the ultra-faint Milky Way satellites: solving the missing satellite problem," *Astrophysical Journal*, vol. 670, no. 1, pp. 313–331, 2007.

[96] S. Koposov, V. Belokurov, N. W. Evans, et al., "The luminosity function of the Milky Way satellites," *Astrophysical Journal*, vol. 686, no. 1, pp. 279–291, 2008.

[97] E. J. Tollerud, J. S. Bullock, L. E. Strigari, and B. Willman, "Hundreds of Milky Way satellites? Luminosity bias in the satellite luminosity function," *Astrophysical Journal*, vol. 688, no. 1, pp. 277–289, 2008.

[98] S. M. Walsh, B. Willman, and H. Jerjen, "The invisibles: a detection algorithm to trace the faintest Milky Way satellites," *Astronomical Journal*, vol. 137, no. 1, pp. 450–469, 2009.

[99] J. Grcevich and M. E. Putman, "H_I in local group dwarf galaxies and stripping by the galactic halo," *Astronomical Journal*, vol. 696, pp. 385–395, 2009.

[100] K. Bernlöhr, O. Carrol, R. Cornils, et al., "The optical system of the H.E.S.S. imaging atmospheric Cherenkov telescopes—part I: layout and components of the system," *Astroparticle Physics*, vol. 20, no. 2, pp. 111–128, 2003.

[101] D. Martínez-Delgado, M. Á. Gómez-Flechoso, A. Aparicio, and R. Carrera, "Tracing out the northern tidal stream of the Sagittarius dwarf spheroidal galaxy," *Astrophysical Journal*, vol. 601, no. 1, part 1, pp. 242–259, 2004.

[102] J. Holder, V. A. Acciari, E. Aliu, et al., "Status of the VERITAS observatory," in *High Energy Gamma-Ray Astronomy: Proceedings of the 4th International Meeting on High Energy Gamma-Ray Astronomy* , F. A. Aharonian, W. Hofmann, and F. Rieger, Eds., vol. 1085 of *American Institute of Physics Conference Series*, pp. 657–660, 2008.

[103] R. Essig, N. Sehgal, and L. E. Strigari, "Bounds on cross sections and lifetimes for dark matter annihilation and decay into charged leptons from gamma-ray observations of dwarf galaxies," *Physical Review D*, vol. 80, no. 2, Article ID 023506, 2009.

[104] J. Bovy, "Substructure boosts to dark matter annihilation from Sommerfeld enhancement," *Physical Review D*, vol. 79, no. 8, Article ID 083539, 2009.

[105] G. D. Martinez, J. S. Bullock, M. Kaplinghat, L. E. Strigari, and R. Trotta, "Indirect dark matter detection from dwarf satellites: joint expectations from astrophysics and supersymmetry," *Journal of Cosmology and Astroparticle Physics*, vol. 6, p. 14, 2009.

[106] L. Pieri, A. Pizzella, E. M. Corsini, E. Dalla Bontà, and F. Bertola, "Could the Fermi Large Area Telescope detect γ-rays from dark matter annihilation in the dwarf galaxies of the local group?" *Astronomy and Astrophysics*, vol. 496, no. 2, pp. 351–360, 2009.

[107] F. Governato, B. Willman, L. Mayer, et al., "Forming disc galaxies in ΛCDM simulations," *Monthly Notices of the Royal Astronomical Society*, vol. 374, no. 4, pp. 1479–1494, 2007.

[108] J. Diemand, P. Madau, and B. Moore, "The distribution and kinematics of early high-σ peaks in present-day haloes: implications for rare objects and old stellar populations," *Monthly Notices of the Royal Astronomical Society*, vol. 364, no. 2, pp. 367–383, 2005.

[109] B. Moore, J. Diemand, P. Madau, M. Zemp, and J. Stadel, "Globular clusters, satellite galaxies and stellar haloes from early dark matter peaks," *Monthly Notices of the Royal Astronomical Society*, vol. 368, no. 2, pp. 563–570, 2006.

[110] L. E. Strigari, S. M. Koushiappas, J. S. Bullock, and M. Kaplinghat, "Precise constraints on the dark matter content of Milky Way dwarf galaxies for gamma-ray experiments," *Physical Review D*, vol. 75, no. 8, Article ID 083526, 2007.

[111] P. Ullio, L. Bergström, J. Edsjö, and C. Lacey, "Cosmological dark matter annihilations into γ rays: a closer look," *Physical Review D*, vol. 66, no. 12, Article ID 123502, 2002.

[112] D. Reed, F. Governato, T. Quinn, J. Gardner, J. Stadel, and G. Lake, "Dark matter subhaloes in numerical simulations," *Monthly Notices of the Royal Astronomical Society*, vol. 359, no. 4, pp. 1537–1548, 2005.

[113] T. Ishiyama, T. Fukushige, and J. Makino, "Variation of the subhalo abundance in dark matter halos," *The Astrophysical Journal*, vol. 696, pp. 2115–2125, 2009.